Published OnlineFirst February 11, 2014; DOI: 10.1158/0008-5472.CAN-13-2990



Cancer Research

# Curative Properties of Noninternalizing Antibody–Drug Conjugates Based on Maytansinoids

Elena Perrino[1], Martina Steiner[1], Nikolaus Krall[1], Gonçalo J.L. Bernardes[1,3,4], Francesca Pretto[2], Giulio Casi[2], and Dario Neri[1]

## Abstract

It is generally thought that the anticancer efficacy of antibody–drug conjugates (ADC) relies on their internalization by cancer cells. However, recent work on an ADC that targets fibronectin in the tumor microenvironment suggests this may not be necessary. The alternatively spliced extra domains A and B (EDA and EDB) of fibronectin offer appealing targets for ADC development, because the antigen is strongly expressed in many solid human tumors and nearly undetectable in normal tissues except for the female reproductive system. In this study, we describe the properties of a set of ADCs based on an antibody targeting the alternatively spliced EDA of fibronectin coupled to one of a set of potent cytotoxic drugs (DM1 or one of two duocarmycin derivatives). The DM1 conjugate SIP(F8)-SS-DM1 mediated potent antitumor activity in mice bearing DM1-sensitive F9 tumors but not DM1-insensitive CT26 tumors. Quantitative biodistribution studies and microscopic analyses confirmed a preferential accumulation of SIP(F8)-SS-DM1 in the subendothelial extracellular matrix of tumors, similar to the pattern observed for unmodified antibody. Notably, we found that treatments were well tolerated at efficacious doses that were fully curative and compatible with pharmaceutical development. Our findings offer a preclinical proof-of-concept for curative ADC targeting the tumor microenvironment that do not rely upon antigen internalization. *Cancer Res; 74(9); 1–10. ©2014 AACR.*

## Introduction

Antibody–drug conjugates (ADC) represent an attractive class of biopharmaceuticals, which has gained considerable attention for the development of anticancer products (1, 2), especially after the approval of drugs such as Adcetris and Kadcyla (3, 4).

It is generally believed that antibodies capable of selective internalization into the tumor cells are needed for efficient ADC development because cytotoxic drugs typically act at the level of intracellular targets. Indeed, it has been claimed that targeting an ADC to a noninternalizing target antigen with the expectation that extracellulary released drug will diffuse into the target cell is not a recipe for a successful ADC (5).

We have recently challenged the concept of a strict requirement for internalization in ADC development. In particular, we have shown that noninternalizing antibodies specific to splice isoforms of fibronectin, coupled to derivatives of cemadotin (a tubulin poison with *in vitro* cytotoxic activity in the 1–20 nmol/L range) are able to mediate a statistically significant tumor growth retardation (albeit at doses as high as 43 mg/kg) in three different murine models of cancer (F9, CT26, and A20; refs. 6, 7). The F8 and the L19 antibodies recognize the alternatively spliced extra domains A and B of fibronectin, respectively, which are markers of tumor angiogenesis (8–10). The fibronectin fibers recognized by the two antibodies are located in the subendothelial extracellular matrix of tumor blood vessels (11). Immunofluorescence and microautoradiographic analysis, following intravenous administration of the L19 and F8 antibodies to tumor-bearing mice, confirmed that the antibodies efficiently and preferentially localized to tumor blood vessels *in vivo*. Quantitative biodistribution studies of antibody uptake are available in tumor-bearing mice (9, 12, 13) and in patients with cancer (14, 15).

With the hope to achieve more potent therapeutic effects, we decided to substitute cemadotin with the maytansinoid derivative DM1 and duocarmycins, highly cytotoxic drugs, which have extensively been used for ADC development with internalizing antibodies.

DM1 is the potent cytotoxic component in trastuzumab-DM1 (Kadcyla), an ADC approved for the treatment of Her2-positive breast cancer (4). DM1 is a maytansinoid derivative, first described in 1992 (16). Maytansinoids are natural products that have been used and investigated in clinical trials (17). They have a macrolide structure based on a 19-membered ring and act by preventing the microtubule polymerization through binding to the same site on the β subunit of tubulin as Vinca

**Authors' Affiliations:** [1]Department of Chemistry and Applied Biosciences, Institute of Pharmaceutical Sciences, ETH Zürich; [2]Philochem AG, Otelfingen, Zurich, Switzerland; [3]Department of Chemistry, University of Cambridge, Cambridge, United Kingdom; and [4]Instituto de Medicina Molecular, Faculdade de Medicina da Universidade de Lisboa, Av. Prof. Egas Moniz, Lisboa, Portugal

**Note:** Supplementary data for this article are available at Cancer Research Online (http://cancerres.aacrjournals.org/).

E. Perrino and M. Steiner contributed equally to this work.

**Corresponding Author:** Dario Neri, ETH Zurich, Vladimir-Prelog-Weg 1-5/10, Zurich 8093, Switzerland. Phone: 41-44-633-7401; Fax: 41-44-633-1358; E-mail: neri@pharma.ethz.ch

**doi:** 10.1158/0008-5472.CAN-13-2990

Published OnlineFirst February 11, 2014; DOI: 10.1158/0008-5472.CAN-13-2990



alkaloids (18). The inhibition of polymerization causes cell-cycle arrest and subsequent apoptosis of the target cell. DM1 has an *in vitro* cytotoxicity that is 3- to 10-fold greater than maytansine and 10- to 200-fold greater than vincristine, a Vinca alkaloid (19, 20).

The other drugs used in this work are derivatives of duocarmycins, antibiotic metabolites isolated from *Streptomyces* bacteria in 1988 (21). Duocarmycins are potent cytotoxic agents with $IC_{50}$ values in the pmol/L range against different cell lines (22). Despite this high potency, duocarmycins themselves are not applicable for cancer chemotherapy because they cause pronounced myelotoxicity, preventing escalation to therapeutically active regimen. The mechanism of action of duocarmycins involves binding to the minor groove of DNA and alkylation of adenines at the N3 position. Their molecular structure shows an indole moiety as DNA-binding component and a spirocyclopropylcyclohexadienone moiety as pharmacophore group that causes sequence-selective DNA alkylation (23). A recent controversial theory claims that duocarmycins act also by inhibiting aldehyde dehydrogenase 1, an enzyme target that plays important roles in the viability and detoxification of cancer cells (24–26). For ADCs applications, we have used duocarmycin analogues that had previously been shown to be more potent and more synthetically accessible than their naturally occurring counterpart (27).

We chose to use antibodies in the small immunoprotein (SIP) format, as we have previously shown that this format combines an excellent uptake at the tumor site with a rapid clearance from blood and normal tissues (9, 28–30).

The SIP format allows the production of ADCs with traceless linkers, i.e., products which regenerate the intact antibody and the intact drug after a suitable cleavage reaction, such as the reduction of a disulfide bond (6) or a hydrolytic process (31). Indeed, the reduction of disulfide bonds connecting antibody and drug is a particularly attractive release mechanism, as it can be triggered by cell death and be further amplified by the release of thiols (e.g., cysteine and glutathione) from dying cells (6).

In this article, we show that SIP(F8), but not the anti-hen egg lysozyme SIP(KSF) antibody used as negative control, is able to preferentially localize on solid tumors at doses of 7 mg/kg, both in the unmodified form and in the ADC form. The conjugate of F8 with DM1 mediated a potent antitumor activity, including several cures, in immunocompetent mice bearing subcutaneously grafted F9 murine teratocarcinomas, but not in mice bearing CT26 tumors. In contrast, only a modest *in vivo* anticancer effect was observed for two F8 derivatives with duocarmycins, despite the fact that the drug was very cytotoxic *in vitro*.

The findings of this article are of potential clinical relevance because the F8 antibody strongly stains the majority of human tumors (9, 32). In contrast, placenta, endometrium, and some vessels in the ovaries were the only structures to be stained by F8 in the triplicate immunofluorescence analysis of a panel of 36 normal adult tissues (33). Noninternalizing ADCs have the ability to induce a potent anticancer activity *in vivo* when used with a suitable payload and may target a broad variety of different malignancies, including lymphomas (34–36) and, potentially, certain leukemias (37).

## Materials and Methods

### Cell culture: cell lines, incubation, and manipulation conditions

Transfected CHO-S cells (Invitrogen) were cultured in suspension in PowerCHO-2CD medium (Lonza) as described before (6). The F9 murine teratocarcinoma cells (American Type Culture Collection, ATCC; CRL-1720) were grown on 0.1% gelatin-coated tissue flasks in Dulbecco's Modified Eagle Medium (Gibco), supplemented with 10% FBS (Gibco), and incubated at 37°C in 5% $CO_2$ atmosphere. The CT26 murine colon carcinoma cells (ATCC; CRL-2638) were cultured in RPMI-1640 (Gibco) supplemented with 10% FBS. Cells were obtained from Invitrogen (CHO-S cells) or ATCC (F9 and CT26 cells) and were kept in culture for less than 6 months after resuscitation. Cell lines undergo comprehensive quality control and authentication procedures by the cell bank before shipment. These include check of post-freeze viability, growth properties and morphology, test for mycoplasma contamination, isoenzyme assay, and sterility test.

### Cytotoxic drugs

The thiol-containing maytansinoid DM1 was obtained from Concortis Biosystems, Corp. The thiomethyl analog S-methyl DM1 was prepared as described before (38). The derivatives of duocarmycins were prepared as described in the Supplementary Data.

### Animals and tumor models

Eleven- to 12-week-old female 129SvEv mice and Balb/c nude mice were obtained from Charles River Laboratories. F9 teratocarcinoma cells ($2.5 \times 10^7$) or CT26 colon carcinoma cells ($5 \times 10^7$) were implanted subcutaneously in the flank. Animals were sacrificed when tumor volumes reached a maximum of 2,000 $mm^3$ or weight loss exceeded 15%. Experiments were performed under project licenses granted by the Veterinäramt des Kantons Zürich (Zürich, Switzerland; 42/2012).

### Cloning, expression, and protein *in vitro* characterization

The gene structure for the F8 antibody in SIP format, the isolation of the KSF antibody, specific to hen egg lysozyme, and the cloning, expression, and characterization of the two antibodies have previously been described (6, 9).

### Antibody–duocarmycin conjugates preparation

Protein solutions were thawed and filtered with a 0.22 $\mu m^2$ filter (Whatman Fp30/02 CA-S) and the concentration (0.4–0.5 mg/mL) was determined by measuring the UV absorbance at 280 nm [protein extinction coefficient at 280 nm: 56,380/(mol/L·cm), estimated using the ExPASy ProtParam tool]. Polypropylene round-bottom tubes (BD Falcon) filled with the protein solution were placed inside a Schlenk flask and degassed by three alternating rounds of vacuum and argon flow. A solution of 0.1 mol/L tris(2-carboxy-ethyl)-phosphine hydrochloride (TCEP•HCl; ABCR) in degassed PBS pH 7.4 was added to 30 molar equivalents over antibody monomer, mixed on a magnetic stirrer for 5 minutes at room temperature and

Published OnlineFirst February 11, 2014; DOI: 10.1158/0008-5472.CAN-13-2990



incubated at 4°C over night, under argon atmosphere. For the purification of the reduced antibodies, a HiPrep desalting column (GE Healthcare) on a AKTA purifier fast protein liquid chromatography (FPLC) system was equilibrated with degassed 50 mmol/L HEPES buffer, containing 5 mmol/L glycine (Fluka), 3% glycerol (v/v; Sigma Aldrich), and 2 mmol/L EDTA (Acros), pH 6.2. The reduced protein solution was injected onto the preequilibrated column and eluted. Fractions of 1 mL of the eluting conjugate were collected manually, with a typical recovery of 75%. The concentration of pooled fractions of purified reduced antibodies was determined by measuring the absorption at 280 nm. Twenty equivalents of duocarmycin derivatives [dimethyl sulfoxide (DMSO; Fluka) stock solutions, c = 0.01 mol/L] over antibody monomer were used for the conjugation in a Schlenk flask, degassed by three alternating rounds of vacuum and argon flow. First, ethylene glycol dimethyl ether (Acros) was added to the antibody solution under vigorous stirring, realizing a 5% final concentration. Subsequently, the DMSO solution of the drugs was added. The reaction was allowed to proceed for 2 hours at room temperature under argon atmosphere. The resulting ADCs were purified from excess drug by FPLC with a HiPrep desalting column, preequilibrated with degassed 50 mmol/L HEPES buffer, pH 7.2 in the case of the carbamate derivative, and pH 6 for the carbonate derivatives, containing 5 mmol/L glycine, 50 mmol/L NaCl (Merck), and 3% glycerol. Fractions containing the conjugates were pooled, snap-frozen in liquid nitrogen and stored at −80°C until further use.

### Antibody–DM1 conjugates preparation

The conjugation of thiol-containing drugs to terminal cysteines of antibodies has been described in detail elsewhere (39). Briefly, the antibody was reduced with 30 equivalents of TCEP•HCl (ABCR) in PBS, pH 7.4, and then modified with 2,500 equivalents over antibody monomer of the Ellman reagent (Sigma-Aldrich). In contrast with previous descriptions, DM1 conjugation required a different buffer system due to relatively poor solubility of the drug. Specifically, the antibody–Ellman conjugate was purified in PBS pH 7.4, containing 5% sucrose (w/v; AppliChem) and 10% N,N-dimethylacetamide (DMA; Acros Organics). Ten equivalents of thiol drug DM1 over antibody monomer were then weighed into a plastic vial and dissolved in DMA immediately before addition to the purified antibody–Ellman conjugate. The reaction was stopped after 5 minutes with the addition of 500 equivalents (relative to the antibody monomer) of iodoacetamide (Sigma-Aldrich). The final ADC was purified by FPLC, using the PBS/sucrose/DMA buffer. ADCs were then concentrated to the desired concentration, snap-frozen in liquid nitrogen and stored at −80°C until further use.

### ADC Characterization

All ADCs were analyzed by SDS–PAGE (Invitrogen), size-exclusion chromatography (Superdex200 10/300GL; GE Healthcare), and protein mass spectrometry. The EDA-binding properties of SIP(F8)-SS-DM1 were analyzed by surface plasmon resonance (BIAcore 3000 System; GE Healthcare; Supplementary Fig. S4) on an EDA-coated CM5 sensor chip (BIAcore) as previously described (6).

### Biodistribution studies

The *in vivo* targeting performance of the antibody–DM1 conjugates was assessed by quantitative biodistribution studies as described before (40). SIP(F8) and the control SIP(KSF) antibody, both in unmodified and ADC form, were radioiodinated with $^{125}$I (PerkinElmer) and injected into the lateral tail vein of immunocompetent 129SvEv mice, bearing subcutaneously grafted F9 tumors (5 mice/group), at the dose of 7 mg/kg (i.e., 177 nmol of ADC/kg of body weight of animal, corresponding to 130 μg of drug/kg of body weight of animal, ∼2.6 μg/injection/mouse). Mice were sacrificed 24 hours after injection, organs were excised, weighed, and radioactivity was measured using a Packard Cobra γ counter. Radioactivity of organs was expressed as percentage of injected dose per gram of tissue (%ID/g ± SEM).

Immunoreactivity of the labeled proteins were confirmed by analyzing the retention of radioiodinated proteins on EDA coupled to CNBr-activated sepharose (GE Healthcare) as previously described (data not shown; ref. 40).

### Immunofluorescence studies of treated tumors

For *ex vivo* detection of the localization of SIP(F8)-SS-DM1, a microscopic analysis was performed. Immunocompetent 129SvEv mice, bearing subcutaneously grafted F9 tumors, were treated with a single injection of 7 mg/kg of the F8 conjugate or of the control KSF conjugate (dose in analogy to the therapy experiment) and sacrificed 24 hours after the injection. Tumors were excised, embedded in cryoembedding medium (Thermo Scientific) and cryostat sections (10 μm) were stained using the following antibodies: rabbit anti-human IgE (Dako Cytomation), to detect the antibodies, and rat anti-mouse CD31 (BD Biosciences) to detect endothelial cells. Anti-rabbit IgG-Alexa Fluor 488 (molecular probes by Life Technologies) and anti-rat IgG-Alexa Fluor 594 (Molecular Probes by Life Technologies) were used as secondary reagents for microscopic detection.

### Therapy studies

When tumors were clearly palpable, 5 to 6 days after subcutaneous tumor implantation, and the tumors typically exhibited a size of 80 to 120 mm$^3$, mice were randomly grouped ($n = 5$) and injected intravenously into the lateral tail vein.

In the study with duocarmycin conjugates and in the first study with DM1 conjugates, mice were injected daily for a period of 7 days, with ADCs, the corresponding free drug or the vehicle. The daily dose of antibody–duocarmycins conjugates was 2.9 mg/kg (i.e., 74 nmol of ADC/kg of body weight of animal, corresponding to 34 μg of drug/kg of body weight of animal, ∼0.7 μg/injection/mouse) for the carbamate derivative and 1.9 mg/kg (i.e., 48 nmol of ADC/kg of body weight of animal, corresponding to 22 μg of drug/kg of body weight of animal, ∼0.44 μg/injection/mouse) in the case of the carbonate derivative, whereas 7 mg/kg was the daily injected dose for DM1 conjugates. Equimolar amounts of the untargeted drugs were also injected.

In the second DM1 conjugate therapy study, mice were injected only three times, in intervals of 72 hours.

Published OnlineFirst February 11, 2014; DOI: 10.1158/0008-5472.CAN-13-2990



The body weight of mice was monitored daily and tumor volumes were measured daily with a digital caliper (volume = length × width$^2$ × 0.5). Results are expressed as volume in mm$^3$ ± SEM. Animals were sacrificed when tumor volumes reached a maximum of 2,000 mm$^3$ or weight loss exceeded 15%.

### Statistical analysis

Data are expressed as mean ± SEM. Differences in tumor volume between therapy groups were compared using GraphPad Prism grouped two-way ANOVA multiple comparisons (Bonferroni corrected) analysis with $P < 0.05$ considered to be significant (GraphPad Software Inc.).

## Results

### ADC preparation and characterization

Figure 1 illustrates the chemical strategies followed for the preparation of ADCs based on DM1 or duocarmycins and on the F8 and KSF antibodies in SIP format.

In both of the cases, disulfide-linked ADCs were produced using a site-specific conjugation strategy (6) based on the direct modification of the C-terminal cysteines present in the antibodies, with potent thiol-containing duocarmycin or DM1 drugs, following a mild reduction of the antibody's C-terminal disulfide with TCEP. In the case of duocarmycin conjugates (Fig. 1A), pyridyldithio drug derivatives were directly reacted with thiol-containing reduced SIP, whereas in the case of DM1 conjugates (Fig. 1B) the C-terminal cysteine was first modified with the Ellman reagent. The subsequent addition of thiol-containing DM1 yielded a homogeneous mixed disulfide–linked ADC. Conjugation reactions proceeded with high conversion (>95%). Figure 2 presents a complete *in vitro* characterization by gel-electrophoresis, size-exclusion chromatography, and ESI-MS (electrospray-mass spectrometry) of all F8-ADCs that were used for the *in vivo* studies. The negative control KSF–ADCs displayed similarly good quality (data not shown). Supplementary Fig. S1 presents an SDS–PAGE analysis of ADCs upon incubation in murine serum at 37°C. Antigen binding of SIP(F8)-SS-DM1 was confirmed by BIAcore analysis (Supplementary Fig. S4).

### Therapy studies in tumor-bearing mice

The therapeutic activity of ADCs based on duocarmycins, containing a disulfide bond and either a carbonate or a carbamate in the linker (Fig. 1A), was tested in immunocompetent 129SvEv mice bearing subcutaneous F9 tumors. Antibody–duocarmycin conjugates exhibited a lower toxicity compared with the free drug *in vivo*. In contrast with the carbamate based ADC, which did not substantially delay tumor growth, statistically significant ($P < 0.0001$, on day 12) tumor growth inhibition was observed for SIP(F8)-SS–duocarmycin with a carbonate linker compared with the saline treatment (Fig. 3). It is worth noting that internalizing ADCs based on similar duocarmycin derivatives have been previously shown promising efficacy in tumor-bearing mice (41).

A completely different performance was observed when SIP (F8)-SS-DM1 was tested in the F9 tumor model. In an initial study, both F8 and KSF ADCs mediated complete and long-lasting tumor eradication, with 7 daily doses at 7 mg/kg, starting when tumors had reached 100 mm$^3$ of volume. No therapeutic activity was observed for the free drug used at equimolar doses (Fig. 4). To see whether a difference in therapeutic activity could be observed between SIP(F8)-SS-DM1 and SIP(KSF)-SS-DM1, the therapy experiment was repeated with only three injections at 7 mg/kg. In this case, SIP(F8)-SS-DM1 continued to exhibit a strong therapeutic activity, whereas all tumors progressed when the KSF counterpart was used (Fig. 4 and Supplementary Fig. S2). In the case

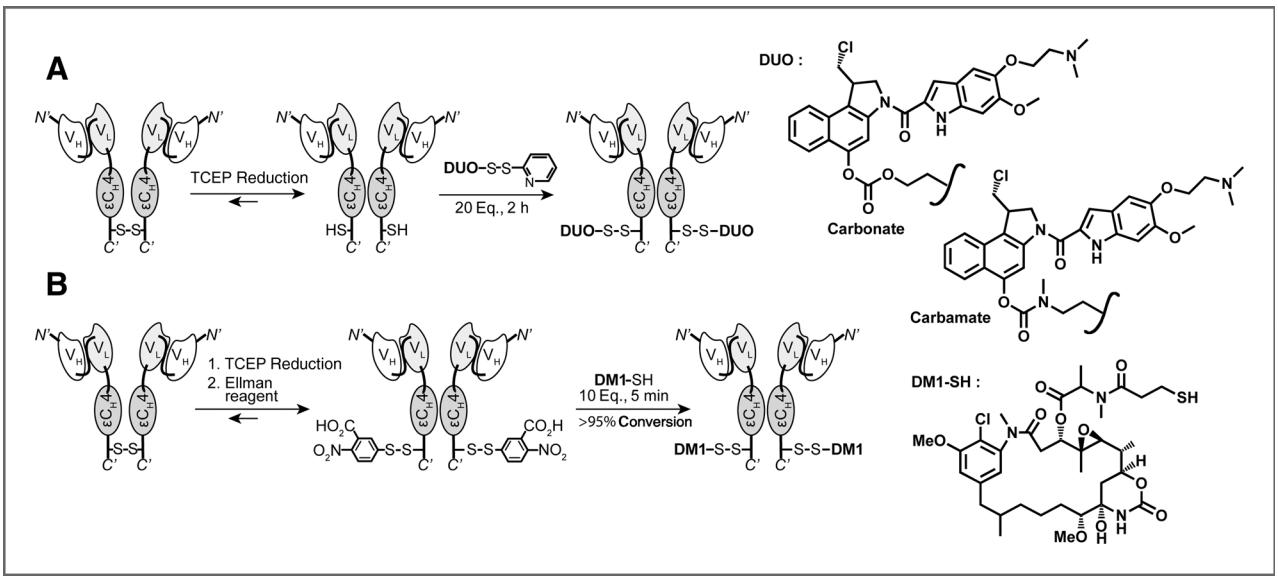


Figure 1. Synthetic scheme for the site-selective modification at the C-terminal cysteine residue of SIP(F8) with duocarmycins (DUO; A) and DM1 (B). The N- and C-termini are indicated with N′ and C′.

Published OnlineFirst February 11, 2014; DOI: 10.1158/0008-5472.CAN-13-2990



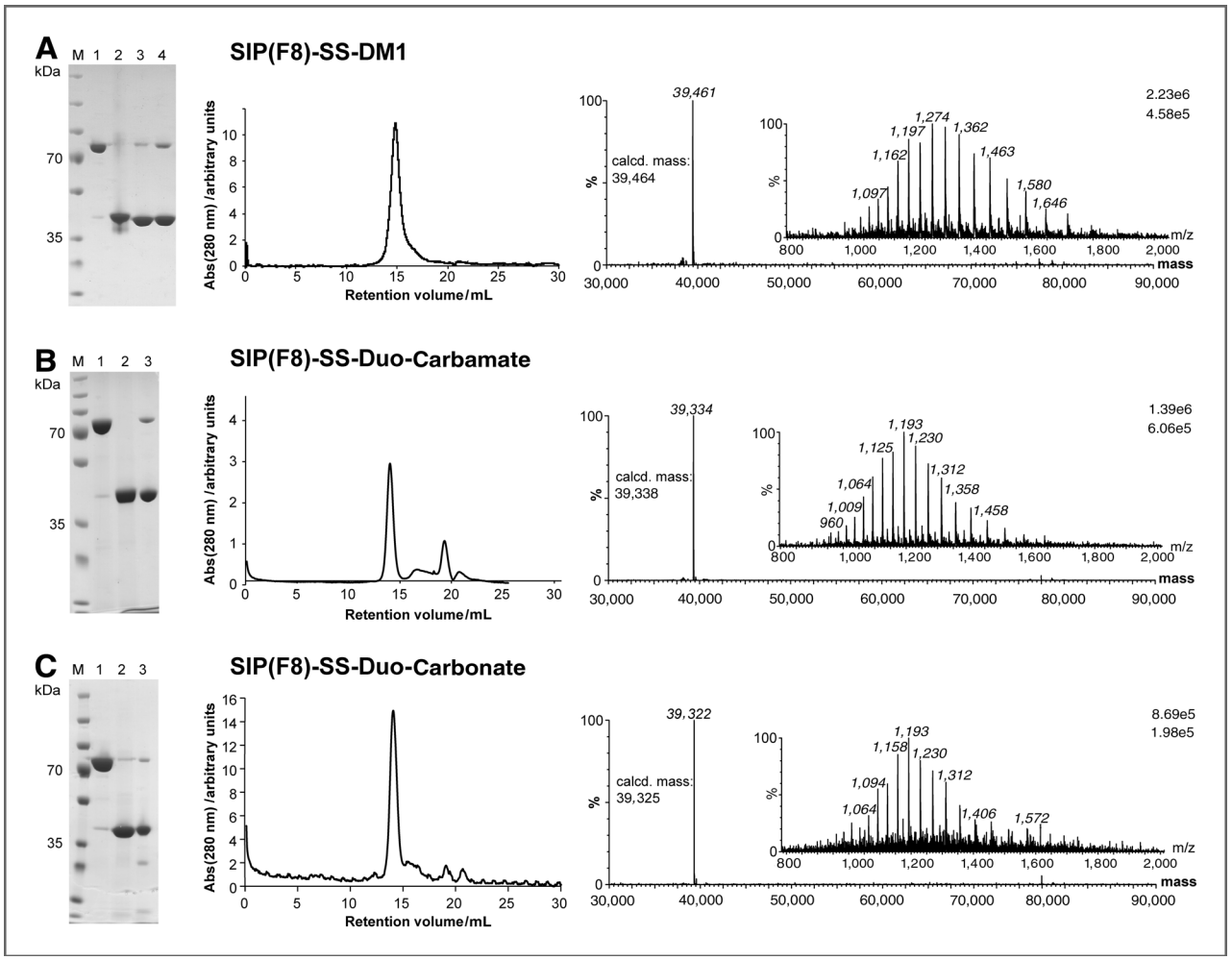


Figure 2. SDS–PAGE monitoring of the SIP(F8) modification process, size-exclusion chromatography analysis, and ESI-MS spectra of the conjugates SIP(F8)-SS-DM1 (A) and SIP(F8)-SS-duocarmycins [with the carbamate (B) or the carbonate (C) in the linker]. In the gels, M is the molecular weight marker; lanes 1 and 2 represent unmodified SIP(F8) in nonreducing and reducing conditions; lane 3 the SIP(F8)-SS-Ellman intermediate (A) or the final duocarmycin conjugate (B and C); lane 4 the final SIP(F8)-SS-DM1 conjugate.

of F8-based ADCs, 3 of 5 mice were cured (i.e., remained tumor-free for >180 days), whereas tumors in the remaining 2 mice started to regrow after day 20.

A worse therapeutic effect was observed in immunocompetent Balb/c mice bearing CT26 murine tumors. Although SIP(F8)-SS-DM1 continued to exhibit superiority compared with saline ($P = 0.0149$, on day 13) and free drug ($P = 0.0020$, on day 13) treatment, no cures were observed. CT26 cells are less sensitive to DM1 ($IC_{50} = 1.6 \times 10^{-8}$ mol/L) compared with F9 cells ($IC_{50} = 2.2 \times 10^{-10}$ mol/L; Supplementary Fig. S3).

### Biodistribution and microscopic analysis in F9 tumor-bearing mice

We performed a quantitative biodistribution experiment (Fig. 5A) in immunocompetent 129SvEv mice, bearing subcutaneously grafted F9 tumors, using intact SIP antibodies or the corresponding DM1 conjugates. Analysis of %ID/g of tissue 24 hours after intravenous administration revealed a preferential accumulation of F8 and F8-DM1 at the tumor site, which was not observed for the negative control KSF antibody and the corresponding KSF–DM1 conjugate.

The results confirmed that the targeting properties of the F8 antibody were preserved at a dose of 7 mg/kg (the same dose of the therapy experiment) and that the conjugation to DM1 did not interfere with tumor targeting.

An *ex vivo* immunofluorescence analysis (Fig. 5B) of tumor sections following intravenous administration of the ADCs products, confirmed the selective accumulation of SIP (F8)-SS-DM1 in the subendothelial extracellular matrix, whereas no selective accumulation was observed for the KSF counterpart.

## Discussion

To our knowledge, this is the first report of the induction of lasting complete remissions in a murine immunocompetent model of cancer, using noninternalizing ADCs.

Published OnlineFirst February 11, 2014; DOI: 10.1158/0008-5472.CAN-13-2990



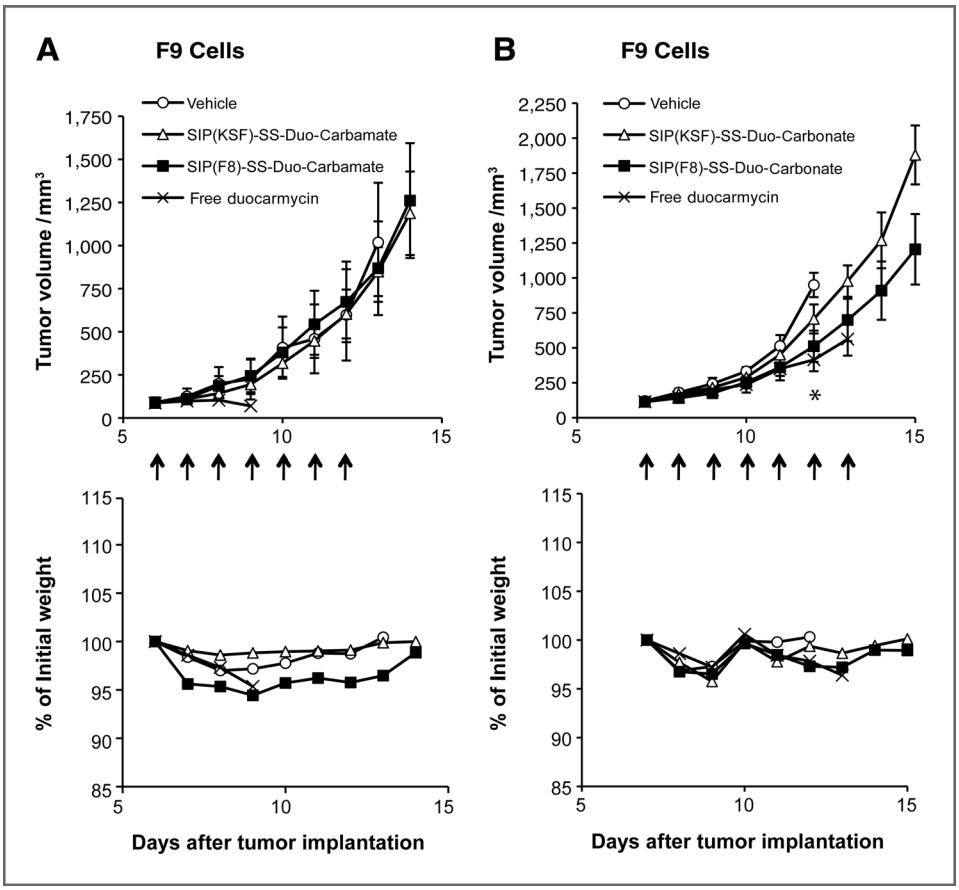


**Figure 3.** Therapeutic activity of SIP(F8)-SS-duocarmycins against F9 teratocarcinoma and analysis of toxicity by the observation of changes in weight of treated mice. When tumors reached 100 $mm^3$ of volume, mice were randomly grouped and intravenously injected daily seven times (arrows) with the vehicle (○), SIP(F8) derivatives (■; A, carbamate at 2.9 mg/kg; B, carbonate at 1.9 mg/kg), the KSF counterparts (Δ), and the free drugs (×; at equimolar doses). Data, mean tumor volumes (±SEM); $n = 5$ mice per group. Mice were checked and weighed every day. *, significant for SIP (F8)-SS-Duo-carbonate versus saline ($P < 0.0001$) on day 12.

The demonstration that cancer cures can be obtained without antibody internalization, by the targeted delivery of a suitable disulfide-linked ADC to the subendothelial extracellular matrix in solid tumors, suggests that a high local concentration of a potent cytotoxic agent close to the tumor neovasculature can mediate an extensive damage to the whole neoplastic mass. Noninternalizing ADCs rely on labile linkers for drug release in close proximity to the target because the intact ADC cannot passively diffuse into cells. Our ADCs are based on linkerless antibody modification with a potent thiol-containing drug, DM1-SH, which affords homogeneous products by formation of a mixed disulfide. Following extravasation, ADCs which have bound to the subendothelial extracellular matrix release the cytotoxic payload and initiate tumor cell death. Dying cells release high concentrations of reducing agents (e.g., cysteine, glutathione) from their intracellular compartments into the surrounding environment, thus, triggering additional release of drug in a self-amplifying fashion.

The striking difference between the potent *in vitro* activity of duocarmycin and the relative lack of activity of the corresponding ADCs *in vivo* suggests that an insufficient stability of the conjugates (Supplementary Fig. S1) and their pro-drug characteristics (a cyclopropyl ring needs to be formed, to display DNA alkylating activity; 23) may cancel the benefit of antibody-based pharmacodelivery.

Disulfide-bound DM1 was found to be a suitable payload for ADC development. The finding that ADCs of irrelevant specificity in the mouse (e.g., SIP(KSF)-SS-DM1) may have a potent antitumor activity (at higher doses compared with the tumor-homing F8-based ADC) is not uncommon in this area of research and may reflect a therapeutic benefit, associated with a slow drug release.

In principle, the antibody-based delivery of potent cytotoxic agents to the modified subendothelial extracellular matrix in tumors should offer a number of advantages, compared with the use of internalizing ADCs. Splice isoforms of fibronectins and tenascins are overexpressed in the majority of malignancies, whereas being undetectable in most normal adult tissues, thus, providing the opportunity to treat different cancer types with the same product. ECM antigens tend to be more stable and more abundant compared with cellular antigens. The release of cytotoxic payload in the extracellular environment may facilitate a by-stander effect, as the drug can diffuse and internalize in neighboring cells.

The F8 antibody cross-reacts between mouse and man, thus, allowing the study of ADC products in syngeneic immunocompetent mouse models of cancer. The intact F8 antibody, in SIP or immunoglobulin G format, does not display any antitumor activity (6, 7) at the doses used (A. Villa, S. Wulhfard, and D. Neri, data not shown). Potentially, SIP(F8)-SS-DM1 could activate an anticancer immunity, a

Published OnlineFirst February 11, 2014; DOI: 10.1158/0008-5472.CAN-13-2990



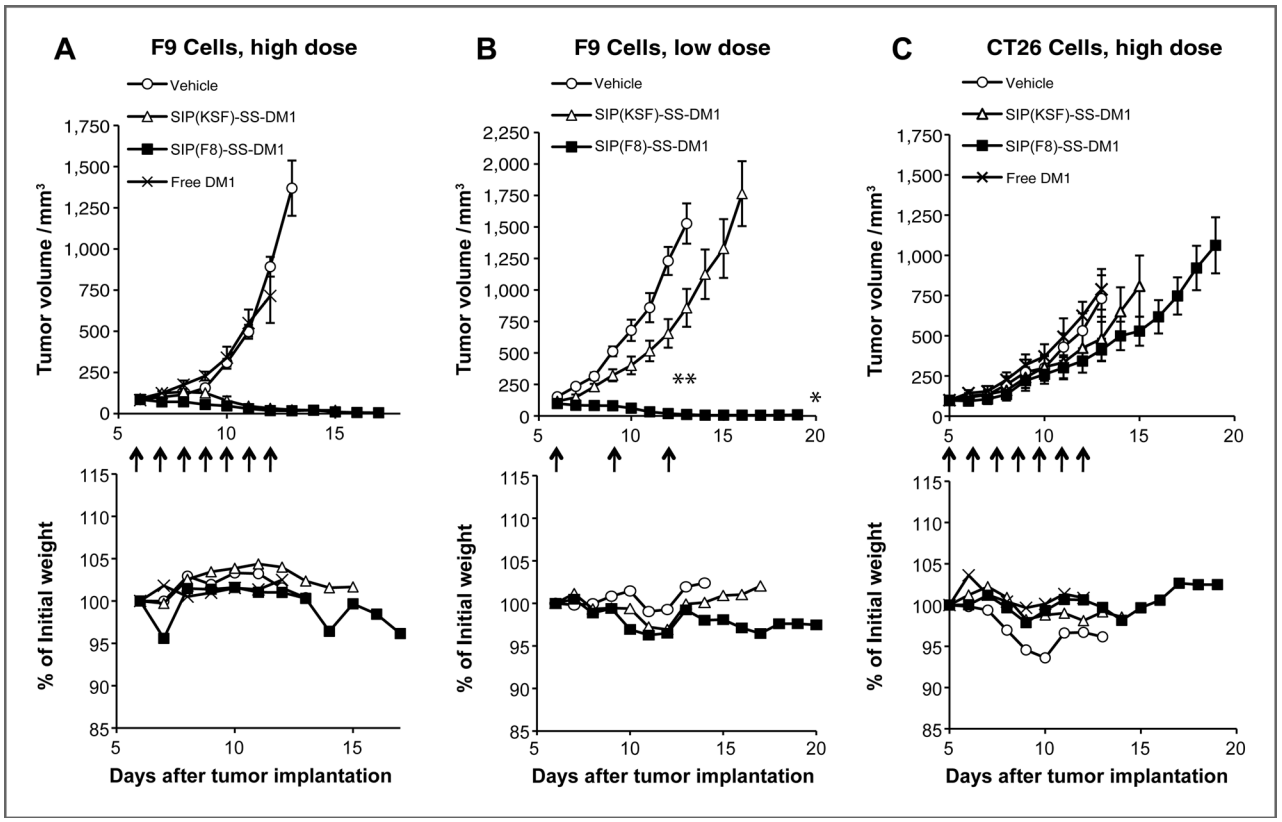


Figure 4. Therapeutic activity of SIP(F8)-SS-DM1 against F9 teratocarcinoma (A and B), against CT26 colon carcinoma (C), and corresponding analysis of toxicity by the observation of changes in weight of treated mice. When tumors reached 100-mm$^3$ volume, mice were randomly grouped and intravenously injected. A and C, mice were injected daily for a period of 7 days; B, mice were injected only three times, every 72 hours, with the vehicle (○), SIP(F8)-SS-DM1 (■), at 7 mg/kg, the KSF counterpart (Δ), and the free drug (×; at equimolar doses). Data, mean tumor volumes (±SEM); $n = 5$ mice per group. Mice were checked and weighed every day. *, 3 of 5 mice were cured and remained tumor-free for >180 days. After day 20, tumors in the remaining two mice started to regrow. **, significant for SIP(F8)-SS-DM1 versus saline ($P = 0.0149$) and versus free drug ($P = 0.0020$) on day 13.

topic which is at present under intense experimental investigation by our laboratory.

Precise knowledge of ADC localization in the tumor (by microscopic analysis; Fig. 5B) and a quantitative understanding of the amount of product that reaches the tumor mass (by biodistribution analysis; Fig. 5A) should provide a rational basis for the comparison of therapeutic efficacy in different models of cancer. Accurate dosimetric studies of tumor-targeting performance in patients, which are possible thanks to advances in antibody radiolabeling procedures (30) and to the implementation of immuno-PET procedures (15, 42), should allow a direct comparison of clinical data with biodistribution results in mice, facilitating product development and translational research.

In mice, the noninternalizing ADC SIP(F8)-SS-DM1 exhibited a biodistribution profile that was similar to the one of the unmodified antibody (Fig. 5A), even when this was used at 50-fold lower doses (9). This observation indicates that the target antigen was not saturated *in vivo* at doses of 7 mg/kg, which are routinely used for ADC therapy applications but are higher than the ones typically used in antibody biodistribution studies.

A potent antitumor activity was observed with SIP(F8)-SS-DM1 in 129SvEv mice bearing F9 teratocarcinoma, but not in Balb/c mice bearing subcutaneously grafted CT26 colorectal tumors. In *in vitro* cytotoxicity assays, the F9 cell line was found to be at least 100-fold more sensitive to the action of the free thiol DM1 and of its alkylated analog than CT26 cells (Supplementary Fig. S3). These data suggest that the tumor cells, rather than the endothelial cells, may be the primary target for ADC activity, despite of the selective accumulation of SIP(F8)-SS-DM1 around tumor blood vessels.

In certain experimental systems, it has been observed that a selective damage to the tumor endothelium may cause an indirect avalanche of tumor cell deaths (43–45). Other derivatives of the F8 antibody (e.g., fusion proteins with cytokines) have been found to be active both against F9 and CT26 tumors (40, 46), suggesting that the different performance of F8-based ADCs may be related to the different biologic activity of the DM1 payload toward the two cell lines. In the future, it will be interesting to see whether this correlation between *in vitro* sensitivity of tumor cells and *in vivo* performance extends to other syngeneic models of cancer.

The findings of this article are of potential clinical significance because various armed antibodies specific to splice isoforms of fibronectin are currently being studied in clinical trials (37, 47–49). The DM1 payload is one of the most widely

Published OnlineFirst February 11, 2014; DOI: 10.1158/0008-5472.CAN-13-2990



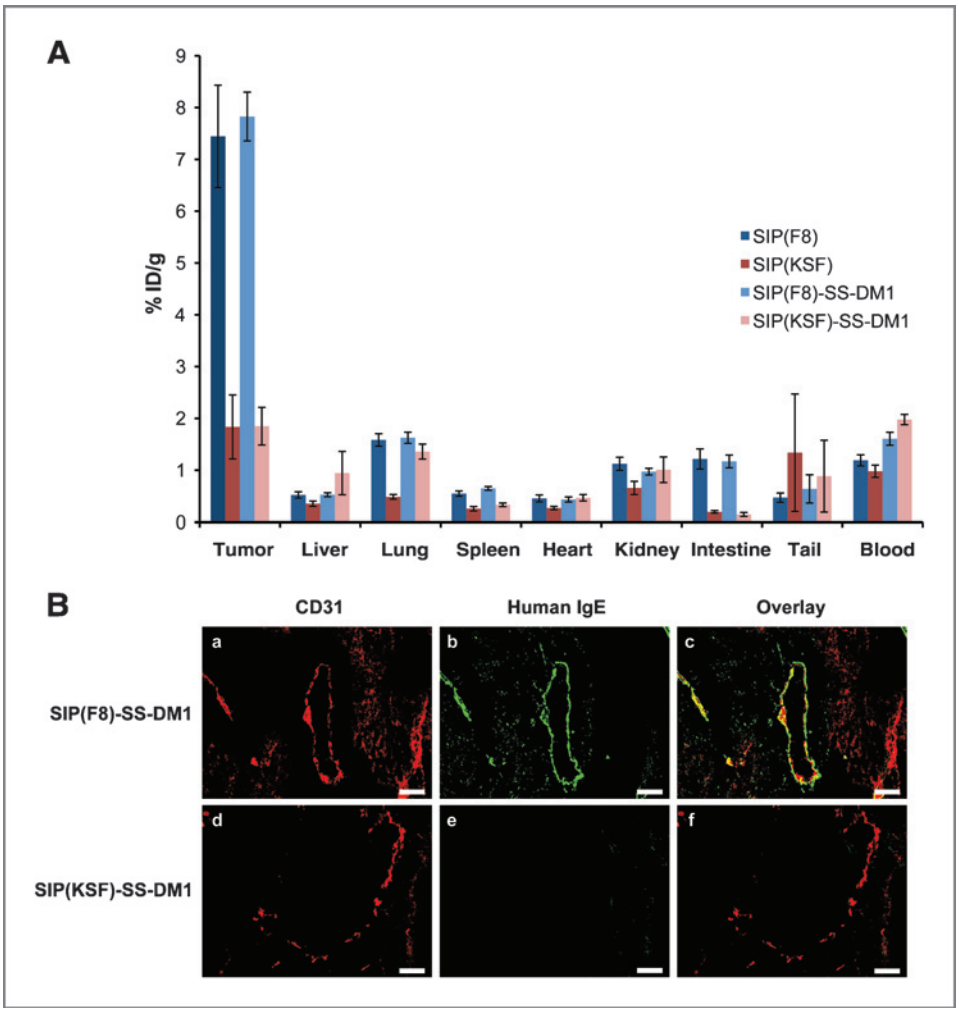


Figure 5. A, biodistribution study of radioiodinated SIP(F8) and SIP (KSF) antibodies, both unmodified and conjugated with DM1, 24 hours after a single intravenous injection (7 mg/kg) into 129SvEv mice bearing F9 tumors. B, immunofluorescence analysis performed on F9 murine teratocarcinoma after a single intravenous injection of SIP(F8)-SS-DM1 (a–c) and SIP(KSF)-SS-DM1 (d–f). Green staining (b and e) represents expression of EDA (staining performed with anti-IgE antibody detecting the εCH4 domain in the recombinant SIP format); red staining (a and d) represents endothelial cells (staining performed with anti-CD31 antibody); c and f, the overlay of red and green fluorescence. Scale bar, 100 μm.

used cytotoxic agents for ADC development (2, 16). It is also a particularly attractive payload because it is detoxified in the liver, helping spare clearance-related organs (50).

## Disclosure of Potential Conflicts of Interest

D. Neri is a consultant/advisory board member and has ownership interest (including patents) in Philogen. No potential conflicts of interest were disclosed by the other authors.

## Authors' Contributions

**Conception and design:** N. Krall, G.J.L. Bernardes, G. Casi, D. Neri
**Development of methodology:** E. Perrino, M. Steiner, N. Krall, G.J.L. Bernardes, G. Casi, D. Neri
**Acquisition of data (provided animals, acquired and managed patients, provided facilities, etc.):** E. Perrino, M. Steiner, G.J.L. Bernardes, F. Pretto
**Analysis and interpretation of data (e.g., statistical analysis, biostatistics, computational analysis):** E. Perrino, M. Steiner, G.J.L. Bernardes, F. Pretto, D. Neri
**Writing, review, and/or revision of the manuscript:** E. Perrino, M. Steiner, N. Krall, G.J.L. Bernardes, G. Casi, D. Neri
**Administrative, technical, or material support (i.e., reporting or organizing data, constructing databases):** D. Neri
**Study supervision:** G. Casi, D. Neri

## Acknowledgments

G.J.L. Bernardes thanks EMBO and Novartis Foundation for generous funding.

## Grant Support

The research work was supported by ETH Zürich, Swiss National Science Foundation, Oncosuisse, Federal Commission from Technology and Innovation (KTI, ADC Project), Japanese-Swiss Science and Technology Cooperation Program, and Philochem AG.

The costs of publication of this article were defrayed in part by the payment of page charges. This article must therefore be hereby marked *advertisement* in accordance with 18 U.S.C. Section 1734 solely to indicate this fact.

Received October 16, 2013; revised January 6, 2014; accepted January 27, 2014; published OnlineFirst February 11, 2014.

## References

1. Chari RV. Targeted cancer therapy: conferring specificity to cytotoxic drugs. Acc Chem Res 2008;41:98–107.
2. Senter PD. Potent antibody drug conjugates for cancer therapy. Curr Opin Chem Biol 2009;13:235–44.

Published OnlineFirst February 11, 2014; DOI: 10.1158/0008-5472.CAN-13-2990




3. Senter PD, Sievers EL. The discovery and development of brentuximab vedotin for use in relapsed Hodgkin lymphoma and systemic anaplastic large cell lymphoma. Nat Biotechnol 2012;30:631–7.
4. Verma S, Miles D, Gianni L, Krop IE, Welslau M, Baselga J, et al. Trastuzumab emtansine for HER2-positive advanced breast cancer. N Engl J Med 2012;367:1783–91.
5. Bander NH. Antibody–drug conjugate target selection: critical factors. Methods Mol Biol 2013;1045:29–40.
6. Bernardes GJL, Casi G, Trussel S, Hartmann I, Schwager K, Scheuermann J, et al. A traceless vascular-targeting antibody–drug conjugate for cancer therapy. Angew Chem Int Ed Engl 2012;51:941–4.
7. Steiner M, Hartmann I, Perrino E, Casi G, Brighton S, Jelesarov I, et al. Spacer length between antibody fold and modified cysteine shapes drug release and therapeutic efficacy of traceless disulfide-linked ADCs targeting the tumor neovasculature. Chemical Science 2012;4: 297–302.
8. Pini A, Viti F, Santucci A, Carnemolla B, Zardi L, Neri P, et al. Design and use of a phage display library. Human antibodies with subnanomolar affinity against a marker of angiogenesis eluted from a two-dimensional gel. J Biol Chem 1998;273:21769–76.
9. Villa A, Trachsel E, Kaspar M, Schliemann C, Sommavilla R, Rybak JN, et al. A high-affinity human monoclonal antibody specific to the alternatively spliced EDA domain of fibronectin efficiently targets tumor neo-vasculature in vivo. Int J Cancer 2008;122:2405–13.
10. Neri D, Bicknell R. Tumour vascular targeting. Nat Rev Cancer 2005;5: 436–46.
11. Niesner U, Halin C, Lozzi L, Gunthert M, Neri P, Wunderli-Allenspach H, et al. Quantitation of the tumor-targeting properties of antibody fragments conjugated to cell-permeating HIV-1 TAT peptides. Bioconjug Chem 2002;13:729–36.
12. Demartis S, Tarli L, Borsi L, Zardi L, Neri D. Selective targeting of tumour neovasculature by a radiohalogenated human antibody fragment specific for the ED-B domain of fibronectin. Eur J Nucl Med 2001;28:534–9.
13. Viti F, Tarli L, Giovannoni L, Zardi L, Neri D. Increased binding affinity and valence of recombinant antibody fragments lead to improved targeting of tumoral angiogenesis. Cancer Res 1999;59: 347–52.
14. Erba PA, Sollini M, Orciuolo E, Traino C, Petrini M, Paganelli G, et al. Radioimmunotherapy with radretumab in patients with relapsed hematologic malignancies. J Nucl Med 2012;53:922–7.
15. Poli GL, Bianchi C, Virotta G, Bettini A, Moretti R, Trachsel E, et al. Radretumab radioimmunotherapy in patients with brain metastasis: a 124 I-L19SIP dosimetric PET study. Cancer Immunol Res 2013;1: 134–43.
16. Chari RV, Martell BA, Gross JL, Cook SB, Shah SA, Blattler WA, et al. Immunoconjugates containing novel maytansinoids: promising anticancer drugs. Cancer Res 1992;52:127–31.
17. Issell BF, Crooke ST. Maytansine. Cancer Treat Rev 1978;5:199–207.
18. Bhattacharyya B, Wolff J. Maytansine binding to the vinblastine sites of tubulin. FEBS Lett 1977;75:159–62.
19. Kovtun YV, Audette CA, Ye Y, Xie H, Ruberti MF, Phinney SJ, et al. Antibody–drug conjugates designed to eradicate tumors with homogeneous and heterogeneous expression of the target antigen. Cancer Res 2006;66:3214–21.
20. Junttila TT, Li G, Parsons K, Phillips GL, Sliwkowski MX. Trastuzumab-DM1 (T-DM1) retains all the mechanisms of action of trastuzumab and efficiently inhibits growth of lapatinib insensitive breast cancer. Breast Cancer Res Treat 2011;128:347–56.
21. Yasuzawa T, Iida T, Muroi K, Ichimura M, Takahashi K, Sano H. Structures of duocarmycins, novel antitumor antibiotics produced by *Streptomyces sp*. Chem Pharm Bull 1988;36:3728–31.
22. Tietze LF, Schmuck K. Prodrugs for targeted tumor therapies: recent developments in ADEPT, GDEPT, and PMT. Curr Pharm Des 2011;17: 3527–47.
23. Hurley LH, Lee CS, McGovren JP, Warpehoski MA, Mitchell MA, Kelly RC, et al. Molecular basis for sequence-specific DNA alkylation by CC-1065. Biochemistry 1988;27:3886–92.
24. Wirth T, Pestel GF, Ganal V, Kirmeier T, Schuberth I, Rein T, et al. The two faces of potent antitumor duocarmycin-based drugs: a structural dissection reveals disparate motifs for DNA versus aldehyde dehydrogenase 1 affinity. Angew Chem Int Ed Engl 2013;52:6921–5.
25. Wirth T, Schmuck K, Tietze LF, Sieber SA. Duocarmycin analogues target aldehyde dehydrogenase 1 in lung cancer cells. Angew Chem Int Ed Engl 2012;51:2874–7.
26. Tercel M, McManaway SP, Leung E, Liyanage HD, Lu GL, Pruijn FB. The cytotoxicity of duocarmycin analogues is mediated through alkylation of DNA, not aldehyde dehydrogenase 1: a comment. Angew Chem Int Ed Engl 2013;52:5442–6.
27. Lajiness JP, Boger DL. Synthesis and characterization of a cyclobutane duocarmycin derivative incorporating the 1,2,10,11-tetrahydro-9H-cyclobuta[c]benzo[e]indol-4-one (CbBI) alkylation subunit. J Am Chem Soc 2010;132:13936–40.
28. Borsi L, Balza E, Bestagno M, Castellani P, Carnemolla B, Biro A, et al. Selective targeting of tumoral vasculature: comparison of different formats of an antibody (L19) to the ED-B domain of fibronectin. Int J Cancer 2002;102:75–85.
29. Berndorff D, Borkowski S, Sieger S, Rother A, Friebe M, Viti F, et al. Radioimmunotherapy of solid tumors by targeting extra domain B fibronectin: identification of the best-suited radioimmunoconjugate. Clin Cancer Res 2005;11:7053s-63s.
30. Tijink BM, Perk LR, Budde M, Stigter-van Walsum M, Visser GW, Kloet RW, et al. (124)I-L19-SIP for immuno-PET imaging of tumour vasculature and guidance of (131)I-L19-SIP radioimmunotherapy. Eur J Nucl Med Mol Imaging 2009;36:1235–44.
31. Casi G, Huguenin-Dezot N, Zuberbuhler K, Scheuermann J, Neri D. Site-specific traceless coupling of potent cytotoxic drugs to recombinant antibodies for pharmacodelivery. J Am Chem Soc 2012;134: 5887–92.
32. Rybak JN, Roesli C, Kaspar M, Villa A, Neri D. The extra-domain A of fibronectin is a vascular marker of solid tumors and metastases. Cancer Res 2007;67:10948–57.
33. Schwager K, Kaspar M, Bootz F, Marcolongo R, Paresce E, Neri D, et al. Preclinical characterization of DEKAVIL (F8-IL10), a novel clinical-stage immunocytokine which inhibits the progression of collagen-induced arthritis. Arthritis Res Ther 2009;11:R142.
34. Sauer S, Erba PA, Petrini M, Menrad A, Giovannoni L, Grana C, et al. Expression of the oncofetal ED-B-containing fibronectin isoform in hematologic tumors enables ED-B-targeted 131I-L19SIP radioimmunotherapy in Hodgkin lymphoma patients. Blood 2009;113: 2265–74.
35. Schliemann C, Palumbo A, Zuberbuhler K, Villa A, Kaspar M, Trachsel E, et al. Complete eradication of human B-cell lymphoma xenografts using rituximab in combination with the immunocytokine L19-IL2. Blood 2009;113:2275–83.
36. Schliemann C, Wiedmer A, Pedretti M, Szczepanowski M, Klapper W, Neri D. Three clinical-stage tumor targeting antibodies reveal differential expression of oncofetal fibronectin and tenascin-C isoforms in human lymphoma. Leuk Res 2009;33:1718–22.
37. Gutbrodt KL, Schliemann C, Giovannoni L, Frey K, Pabst T, Klapper W, et al. Antibody-based delivery of interleukin-2 to neovasculature has potent activity against acute myeloid leukemia. Sci Transl Med 2013;5:201ra118.
38. Lopus M, Oroudjev E, Wilson L, Wilhelm S, Widdison W, Chari R, et al. Maytansine and cellular metabolites of antibody-maytansinoid conjugates strongly suppress microtubule dynamics by binding to microtubules. Mol Cancer Ther 2010;9:2689–99.
39. Bernardes GJL, Steiner M, Hartmann I, Neri D, Casi G. Site-specific chemical modification of antibody fragments using traceless cleavable linkers. Nat Protoc 2013;8:2079–89.
40. Pasche N, Woytschak J, Wulhfard S, Villa A, Frey K, Neri D. Cloning and characterization of novel tumor-targeting immunocytokines based on murine IL7. J Biotechnol 2011;154:84–92.
41. Beck A, Senter P, Chari R. World antibody–drug conjugate submmit Europe: February 21–23, 2011, Frankfurt, Germany. MAbs 2011;3:331–7.
42. Heuveling DA, de Bree R, Vugts DJ, Huisman MC, Giovannoni L, Hoekstra OS, et al. Phase 0 microdosing PET study using the human mini antibody F16SIP in head and neck cancer patients. J Nucl Med 2013;54:397–401.

Published OnlineFirst February 11, 2014; DOI: 10.1158/0008-5472.CAN-13-2990




43. Huang X, Molema G, King S, Watkins L, Edgington TS, Thorpe PE. Tumor infarction in mice by antibody-directed targeting of tissue factor to tumor vasculature. Science 1997;275:547–50.
44. Palumbo A, Hauler F, Dziunycz P, Schwager K, Soltermann A, Pretto F, et al. A chemically modified antibody mediates complete eradication of tumours by selective disruption of tumour blood vessels. Br J Cancer 2011;104:1106–15.
45. Nilsson F, Kosmehl H, Zardi L, Neri D. Targeted delivery of tissue factor to the ED-B domain of fibronectin, a marker of angiogenesis, mediates the infarction of solid tumors in mice. Cancer Res 2001;61:711–6.
46. Hemmerle T, Neri D. The antibody-based targeted delivery of interleukin-4 and 12 to the tumor neovasculature eradicates tumors in three mouse models of cancer. Int J Cancer 2014;134:467–77
47. Johannsen M, Spitaleri G, Curigliano G, Roigas J, Weikert S, Kempkensteffen C, et al. The tumour-targeting human L19-IL2 immunocytokine: preclinical safety studies, phase I clinical trial in patients with solid tumours and expansion into patients with advanced renal cell carcinoma. Eur J Cancer 2010;46:2926–35.
48. Eigentler TK, Weide B, de Braud F, Spitaleri G, Romanini A, Pflugfelder A, et al. A dose-escalation and signal-generating study of the immunocytokine L19-IL2 in combination with dacarbazine for the therapy of patients with metastatic melanoma. Clin Cancer Res 2011;17:7732–42.
49. De Braud FG, Catania C, Masini C, Maur M, Cascinu S, Berardi R, et al. Combinations of the immunocytokine F16-Il2 with doxorubicin or with paclitaxel investigated in phase Ib studies in patients with advanced solid tumors. J Clin Oncol 2010;28:13017.
50. Sun X, Widdison W, Mayo M, Wilhelm S, Leece B, Chari R, et al. Design of antibody–maytansinoid conjugates allows for efficient detoxification via liver metabolism. Bioconjug Chem 2011;22:728–35.

Cancer Research
The Journal of Cancer Research (1916–1930) | The American Journal of Cancer (1931–1940)

AACR American Association for Cancer Research

# Curative Properties of Noninternalizing Antibody–Drug Conjugates Based on Maytansinoids

Elena Perrino, Martina Steiner, Nikolaus Krall, et al.

*Cancer Res* Published OnlineFirst February 11, 2014.